LBL-16212
Preprint c.2

Lawrence Berkeley Laboratory

UNIVERSITY OF CALIFORNIA

RECEIVED
LAWRENCE
BERKELEY LABORATORY
AUG 3 1983
LIBRARY AND
DOCUMENTS SECTION

Materials & Molecular Research Division

Submitted to the Journal of the Electrochemical Society

MATHEMATICAL MODELING OF LIQUID-JUNCTION PHOTOVOLTAIC CELLS: III. OPTIMIZATION OF CELL CONFIGURATIONS

M.E. Orazem and J. Newman

June 1983

TWO-WEEK LOAN COPY

This is a Library Circulating Copy which may be borrowed for two weeks. For a personal retention copy, call Tech. Info. Division, Ext. 6782.

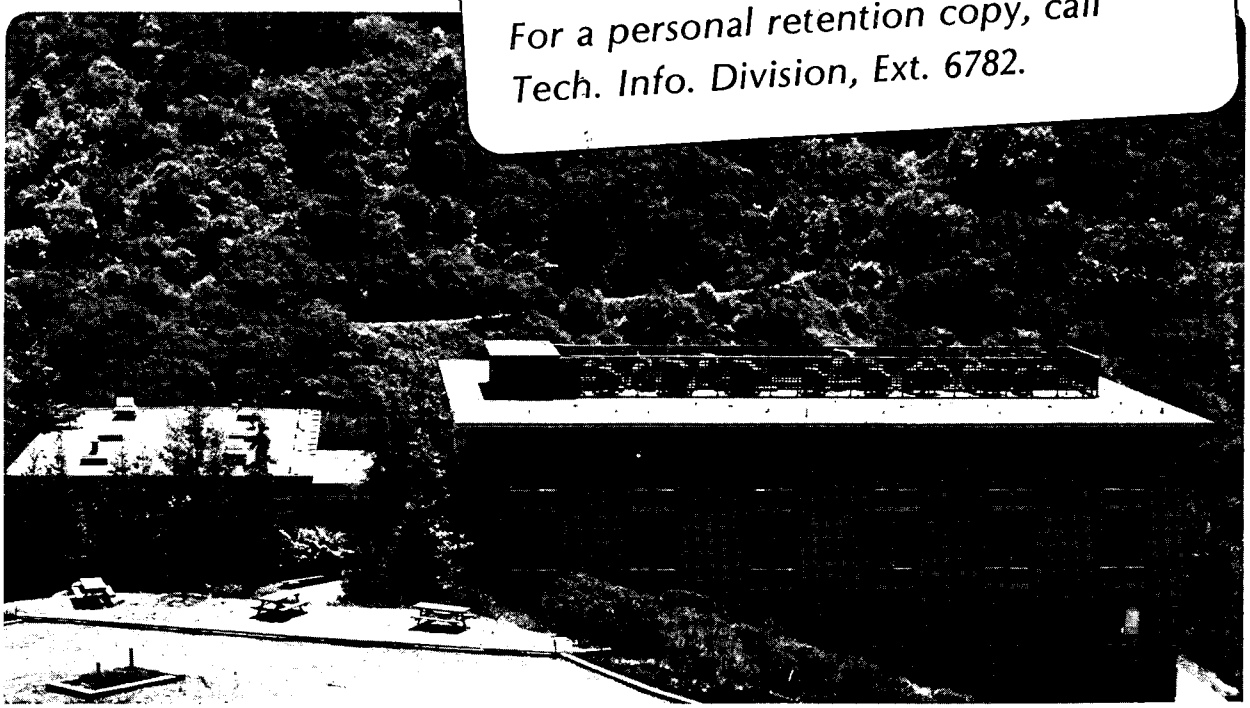

LBL-16212 c.2

Prepared for the U.S. Department of Energy under Contract DE-AC03-76SF00098

DISCLAIMER

This document was prepared as an account of work sponsored by the United States Government. While this document is believed to contain correct information, neither the United States Government nor any agency thereof, nor the Regents of the University of California, nor any of their employees, makes any warranty, express or implied, or assumes any legal responsibility for the accuracy, completeness, or usefulness of any information, apparatus, product, or process disclosed, or represents that its use would not infringe privately owned rights. Reference herein to any specific commercial product, process, or service by its trade name, trademark, manufacturer, or otherwise, does not necessarily constitute or imply its endorsement, recommendation, or favoring by the United States Government or any agency thereof, or the Regents of the University of California. The views and opinions of authors expressed herein do not necessarily state or reflect those of the United States Government or any agency thereof or the Regents of the University of California.

LBL-16212

Mathematical Modeling of Liquid-Junction Photovoltaic Cells:

III. Optimization of Cell Configurations

Mark E. Orazem and John Newman

Materials and Molecular Research Division, Lawrence Berkeley Laboratory, and Department of Chemical Engineering, University of California, Berkeley, California 94720

June 1983

ABSTRACT

The liquid-junction photovoltaic cell is an electrochemical system with one or two semiconducting electrodes. This system provides a means of converting solar energy to chemical or electrical energy. A one-dimensional mathematical model of the liquid-junction photovoltaic cell has been developed. The one-dimensional model of the liquid-junction cell was coupled with primary resistance calculations to predict the optimal performance of three cell configurations. Two cells are considered in which the semiconductor is illuminated from the electrolyte side and one in which the semiconductor is illuminated from the current-collector side. An economic analysis is presented based upon these results. The performance of the liquid-junction photovoltaic cell is dependent upon the design, surface area, and placement of the counterelectrode and current collectors.

Key words: Semiconductor, Solar, Energy Conversion, Economics.

Most studies of the liquid-junction photovoltaic cell have been oriented toward developing an understanding of the semiconducting electrode which characterizes the cell (see, e.g., references 1-19). This work describes the design and optimization of liquid-junction photovoltaic devices. The advantages and problems inherent in the liquid-junction cell are reviewed, and a mathematical model of the liquid-junction cell[20,21] is used to predict the optimal performance of various cell configurations. An economic analysis is presented based upon these results.

1. INTRODUCTION

The liquid-junction photovoltaic cell has appeal because, in contrast to solid-state junctions, the junction between electrolyte and semiconductor is formed easily and allows use of polycrystalline semiconductors. The electrochemical nature of the cell allows both production of electricity and generation of chemical products which can be separated, stored, and recombined to recover the stored energy. These features could make the liquid-junction cell an economical alternative to solid-state photovoltaic devices for solar energy conversion.

Liquid-junction cells also have the advantages that are attributed to other photovoltaic devices. Photovoltaic power plants can provide local generation of power on a small scale. The efficiency and cost of solar cells is independent of scale, and overall efficiency is improved by locating the power plant next to the load. Nuclear and fossil-fuel burning plants, in contrast, are economical only if built on a large scale (on the order of 1000 megawatts).[22]

The design of a liquid-junction photovoltaic cell requires selection of an appropriate semiconductor-electrolyte combination and design of an

efficient cell configuration. The selection of a semiconductor is based upon the band gap, which provides an upper limit to the conversion efficiency of the device, and the choice of electrolyte is governed by the need to limit corrosion. The optimal design of the liquid-junction photovoltaic cell is aided by use of mathematical models.

1.1. Band Gap

Photovoltaic cells rely on the unique properties of semiconductors to convert incident radiation to electrical current. The semiconductor property of interest is the moderate gap between the valence and the conduction-band energy levels. Incident photons of light with energy greater than or equal to the band-gap energy transfer their energy to valence-band electrons, producing conduction-band electrons and vacancies in the valence band.

An upper limit to the efficiency of photovoltaic devices can be established, based upon the band gap and the solar spectrum, without consideration of cell configuration. This "ultimate efficiency" is given by[11]

$$\eta_{ult} = \frac{E_g \int_{E_g}^{\infty} N(E)\, dE}{\int_{0}^{\infty} E\, N(E)\, dE} \tag{1}$$

where E_g is the semiconductor band-gap energy, E is the photon energy, and $N(E)$ is the number density of incident photons with energy E. The fraction of the power in the solar spectrum that can be converted to electrical power is a function of the band gap of the semiconductor. Photons with energy less than the band gap cannot produce electron-hole pairs. Photons with energy greater than the band gap yield the band gap energy.[23-25]

The "ultimate efficiency" of Equation (1) represents an upper limit to conversion of solar energy;[11,26,27] factors such as reflection and absorption losses of sunlight, kinetic and mass transfer limitations, and recombination will reduce the efficiency. These effects are included in section 2.2. A band gap between 1.0 and 1.5 eV is generally considered to be appropriate for efficient conversion of solar energy.

1.2. Corrosion

The application of liquid-junction technology to photovoltaic power conversion is limited by problems associated with the semiconductor-electrolyte interface. Primary among these problems is corrosion. Efficient conversion of solar energy requires a band gap between 1.0 and 1.5 eV, and most semiconductors near this band gap corrode readily under illumination. Semiconductors with large band-gaps (4 to 5 eV) tend to be more stable but cannot convert most of the solar spectrum.

Among the approaches taken to solve this problem, the most successful concern the matching of an electrolyte to the semiconductor. The rate of corrosion is reduced if the semiconductor is in equilibrium with the corrosion products. The rate of corrosion can also be reduced by using a redox couple which oxidizes easily. The oxidation of the redox couple Se_{x+1}^{2-}/Se_x^{2-}, for example, has been shown to compete successfully with photocorrosion reactions for holes in n-type GaAs electrodes.[8,28]

P-type semiconductors used as cathodes are more stable than the more common and generally more efficient n-type semiconducting anodes. The inefficiency of p-type photocathodes has been attributed to the presence of surface states near the valence band energy. A stable p-type photocathode has been developed, however, with a solar conversion efficiency of 11.5

percent.[29] Protective films have been proposed to be a solution to electrode corrosion. The electrode, in this case, would be a small band-gap semiconductor covered by a film composed of either a more stable large band-gap semiconductor, a conductive polymer, or a metal. A large Schottky barrier is frequently present at such semiconductor-metal and semiconductor-semiconductor interfaces which blocks the flux of holes from the semiconductor to the electrolyte. In cases where the photocurrent is not blocked, corrosion can take place between the semiconductor and the protective film.[17,30] Menezes *et al.*[31] discuss the difficulties in avoiding absorptive losses in the metal film while maintaining sufficient integrity to serve the semiconductor corrosion protection function. Frese *et al.*[32] have, however, reported a measurable improvement in the stability of GaAs with less than a monolayer gold metal coverage. Thin conductive poly-pyrrole films appear to be successful in inhibiting corrosion in some electrolytes.[33-38] In addition, insulating polymer films deposited on grain boundaries can improve the performance of polycrystalline semiconductors by reducing surface recombination rates.[39]

1.3. Mathematical Model

Development of a mathematical model constitutes an important step toward design and optimization of the liquid-junction photovoltaic cell. A one-dimensional mathematical model has been developed[20,21] which treats explicitly the semiconductor, the electrolyte, and the semiconductor-electrolyte interface in terms of potentials and concentrations of charged species. The model incorporates macroscopic transport equations in the bulk of the semiconductor and electrolyte. Homogeneous and heterogeneous recombination of electron-hole pairs is included within the

model. Recombination takes place at the semiconductor-electrolyte interface through interfacial sites, which can enhance the recombination rate. Surface sites at the semiconductor-metal interface were not included within the model.

The coupled nonlinear ordinary differential equations of the model were posed in finite-difference form and solved numerically. The mathematical model can be used to gain insight into the operation of cells with semiconducting electrodes, and to optimize their design. The model was used here to calculate the effect of cell design on the performance of an n-type GaAs semiconducting anode in contact with an 0.8 M K_2Se, 0.1 M K_2Se_2, 1.0 M KOH electrolytic solution. The choice of this semiconducting electrode system was based upon the work of Heller and associates.[8,40-42] Cell design parameters are presented in Table 1, and the parameters used in modeling the liquid-junction cell are presented elesewhere.[20,43]

2. CELL CONFIGURATION

The optimal design of liquid-junction photovoltaic cells shares constraints with solid-state photovoltaic cells.[44,45] Current collectors cast

Table 1. Counterelectrode Parameters

Diffusion-Limited Current Density	$i_{3,lim}$	20.0 mA/cm^2
	$i_{4,lim}$	80.0 mA/cm^2
Exchange Current Density	i_o	100.0 mA/cm^2

shadows and can reduce the amount of sunlight absorbed in the semiconductor. A constraint unique to the liquid-junction cell is the placement of the counterelectrode relative to the semiconductor-electrolyte interface. Mass-transfer and kinetic limitations at the counterelectrode and resistance of the electrolyte can play important roles in the optimal design of the liquid-junction photovoltaic cell. These considerations are treated qualitatively by Parkinson.[46]

Under electrolyte-side illumination and without illumination losses, interfacial kinetic limitations, electrolyte resistance, and counterelectrode limitations, the maximum power efficiency of the cell was calculated[43] to be 15.3 percent. The corresponding value under back (or current-collector) side illumination was calculated[43] to be 17.2 percent. These are the values that one might calculate using a potential drop measured between the semiconductor electrode and a reference electrode reversible to the redox reaction and located just outside the diffusion region. The resistance of the electrolyte, illumination losses, and mass-transfer and kinetic limitations at the counterelectrode affect these values and are influenced by cell design. The difference between front and back illumination is due to the assumption that facilitated recombination does not take place at the semiconductor-current collector interface.

The performance of three cell configurations was calculated for operation under AM-2 solar illumination (882 W/m^2). The semiconductor was assumed to be in the form of a thin film (see Mitchell for a review of thin-film photovoltaic technologies[47]). Interfacial kinetic limitations were not included.[20,43] The one-dimensional model of the liquid-junction cell was coupled with the resistance to current flow associated with the two-

dimensional systems. Some methods for calculation of this resistance were reviewed by Fleck *et al.*[48]

2.1. System 1: Wire Counterelectrode

The liquid-junction photovoltaic cell with a wire-grid counterelectrode is presented in Figure 1a. The cell consists of a semiconductive film supported on a metallic current collector, a wire-grid counterelectrode, and a transparent glass cover plate. The space between the cover plate and the semiconductor is filled with the electrolyte. The glass plate is an essential part of the cell because it keeps the system clean and allows optimal orientation of the cell for collection of sunlight. This cell is designed for conversion of solar energy into electrical energy; no provision is made for separation of chemical products. A two-dimensional representation of the cell is presented in Figure 1b.

Sunlight absorbed in the semiconductor must pass through the cover plate, past the counterelectrode, and through the electrolyte. Reflection at each of the interfaces (air-glass, glass-electrolyte, and electrolyte-semiconductor), absorption in the glass and electrolyte, and screening by the counterelectrode decrease the amount of light which can be used for generation of electron-hole pairs. Absorption losses in the electrolyte can be limited by maintaining a small gap between the counterelectrode and the semiconductor. A wide spacing of counterelectrode elements reduces the screening of the semiconductor but also increases the influence of kinetic and mass-transfer effects at the counterelectrode as well as ohmic drop.

The one-dimensional model of the liquid-junction photovoltaic cell was used with averaged uniform current density and solar flux. The shadow of the counterelectrode was implicitly assumed to be diffuse. Resistive losses

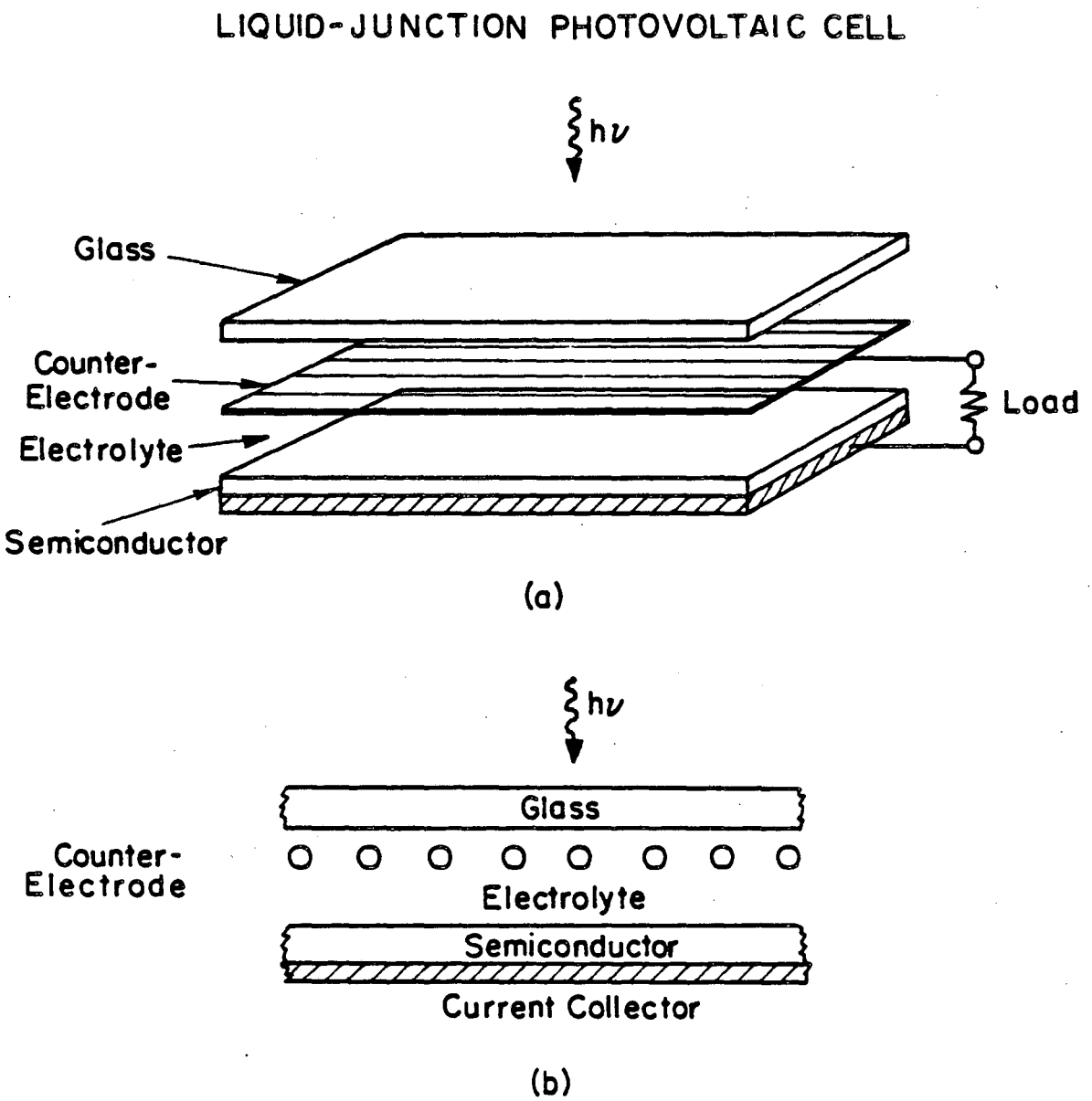

XBL 835-9622

Figure 1. Design of the liquid-junction photovoltaic cell.
System 1: wire counterelectrode.

in the electrolyte were calculated from a two-dimensional solution of Laplace's equation.[49-53] The potential drop in the electrolyte was given by equation (14) in reference 53. The current density at the counterelectrode was assumed to be uniform and was related to the semiconductor current density by

$$i_{ce} = i_{sc} \left(\frac{L}{\pi D}\right), \tag{2}$$

and the counterelectrode shadow was assumed to reduce the magnitude of incident light by a factor of $(1-D/L)$. The effective solar flux was therefore given by

$$q_{sc} = q_o\left(1 - \frac{D}{L}\right)(1 - \rho_{air-glass})e^{-(mx)_{glass}} (1 - \rho_{glass-soln})e^{-(mx)_{soln}}(1 - \rho_{soln-sc}), \tag{3}$$

where ρ_{j-k} is the reflectance associated with the interface $j-k$ and m is the extinction coefficient for a given phase of depth x.

The design parameter for this cell design is the ratio of the counterelectrode element spacing to the counterelectrode element diameter, L/D. When L/D has a value of one, the semiconductor is completely shaded from illumination; when L/D is very large, counterelectrode limitations dominate.

The power density of the cell with a counterelectrode radius of 0.05 cm is presented in Figure 2 as a function of current density with L/D as a parameter. The maximum power density is presented in Figure 3 as a function of L/D. The separation between the cover plate and the counterelectrode was 0.5 cm, and the separation between the semiconductor and the counterelectrode was 0.5 cm. The electrolyte depth was therefore 1.1 cm. The optimal value of L/D is 14, and the maximum power density obtained is 63.5 W/m^2. The current density under the optimal

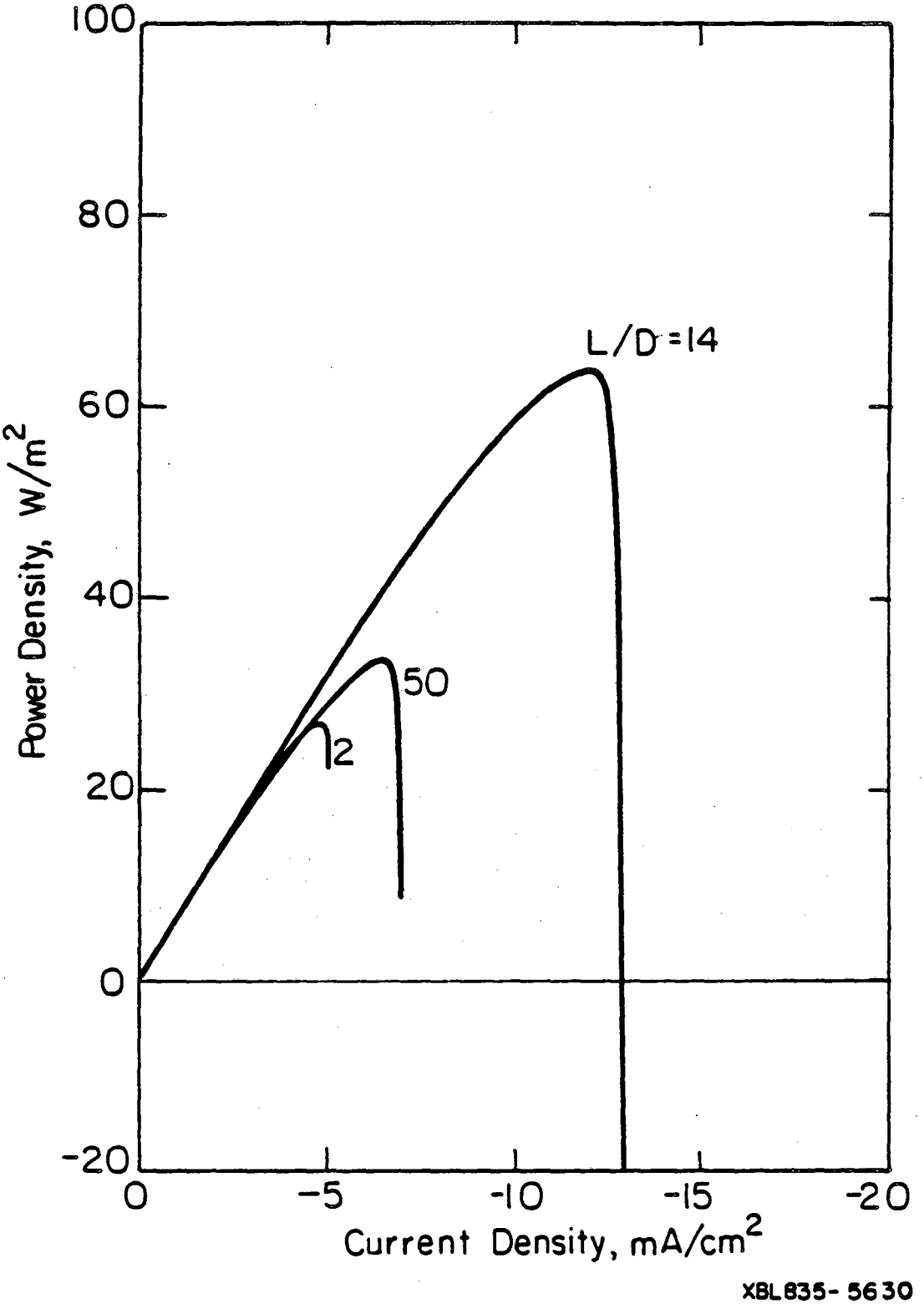

Figure 2. Power density as a function of current density for system 1 with a counterelectrode element diameter of 0.10 cm.

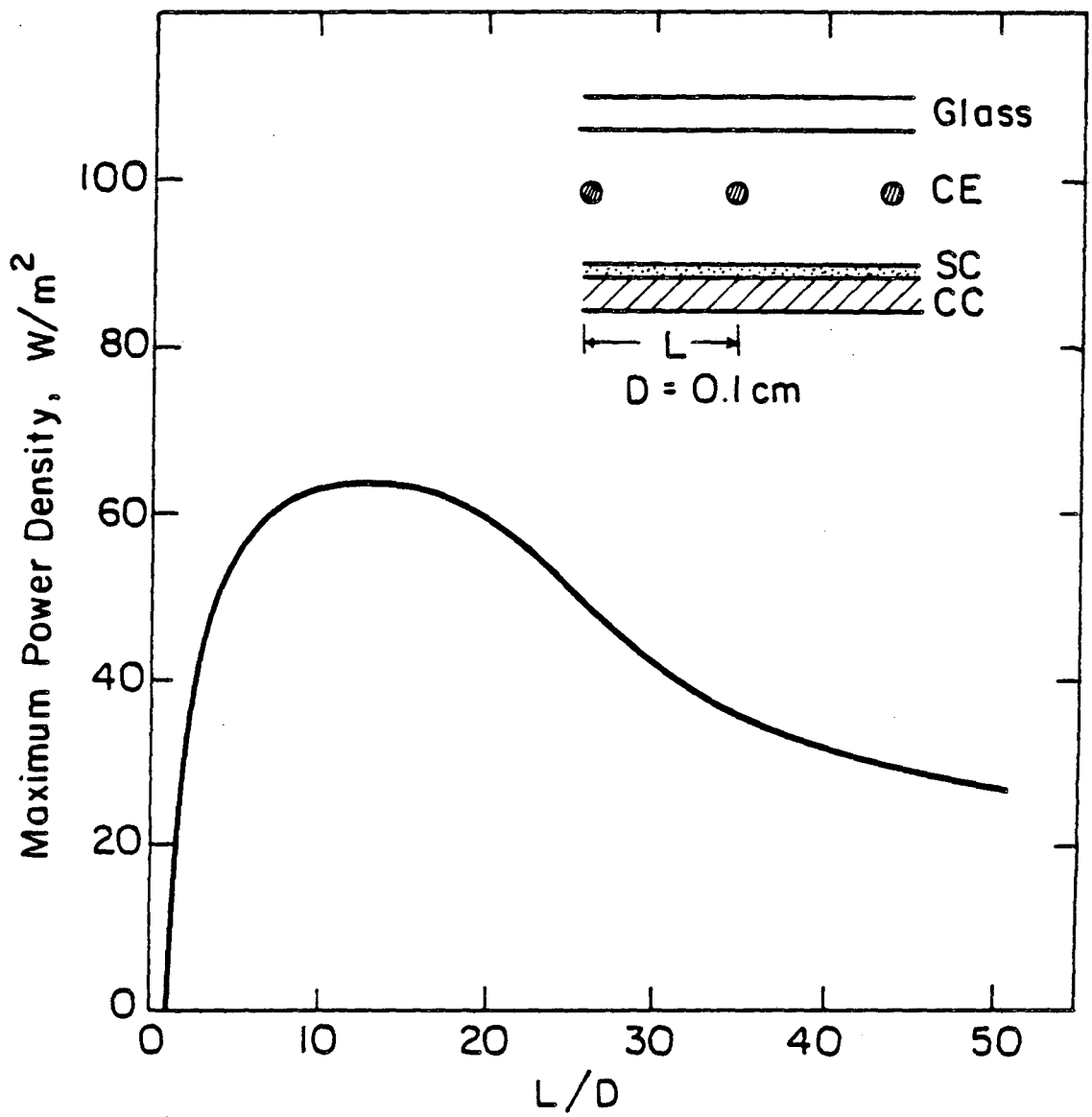

XBL 835-9616

Figure 3. Maximum power density as a function of L/D for system 1 with a counterelectrode element diameter of 0.10 cm.

condition is 11.8 mA/cm^2 delivered at a cell potential of 538.7 mV. The maximum power efficiency of the wire-counterelectrode cell was 7.2 percent.

Kinetic limitations at the counterelectrode further reduce this efficiency. An exchange current density of 1 mA/cm^2 leads to a 5.5 percent power efficiency at an optimal L/D of 10.

2.2. System 2: Slotted Semiconductor

The liquid-junction cell configuration with a slotted-semiconductor electrode is presented in Figure 4. A glass cover plate protects the cell. Sunlight passes through the cover plate and the electrolyte to illuminate the semiconductor surface. Electrical current passes between the semiconductor and the counterelectrode through slots cut in the semiconductor. This configuration has the advantage that no shadows are cast upon the semiconductor; furthermore reaction products could be separated if a membrane were placed between the semiconductor and the counterelectrode.

The primary current distribution and the resistance of a cell containing a slotted electrode were calculated using numerical methods coupled with the Schwarz-Christoffel transformation.[20,54] The cell resistance is a function of three geometric ratios, chosen to be t/G, h/G, and L/h where L is the half-length of the protruding electrode assembly, t is the thickness of the protruding electrode assembly, G is the half-gap between the electrode assemblies, and h is the separation between the electrode and the upper insulating wall. h is also the separation between the counterelectrode and the lower edge of the semiconductor-electrode assembly.

The performance of this cell is a function of four geometric parameters. The distance between the counterelectrode and the semiconductor

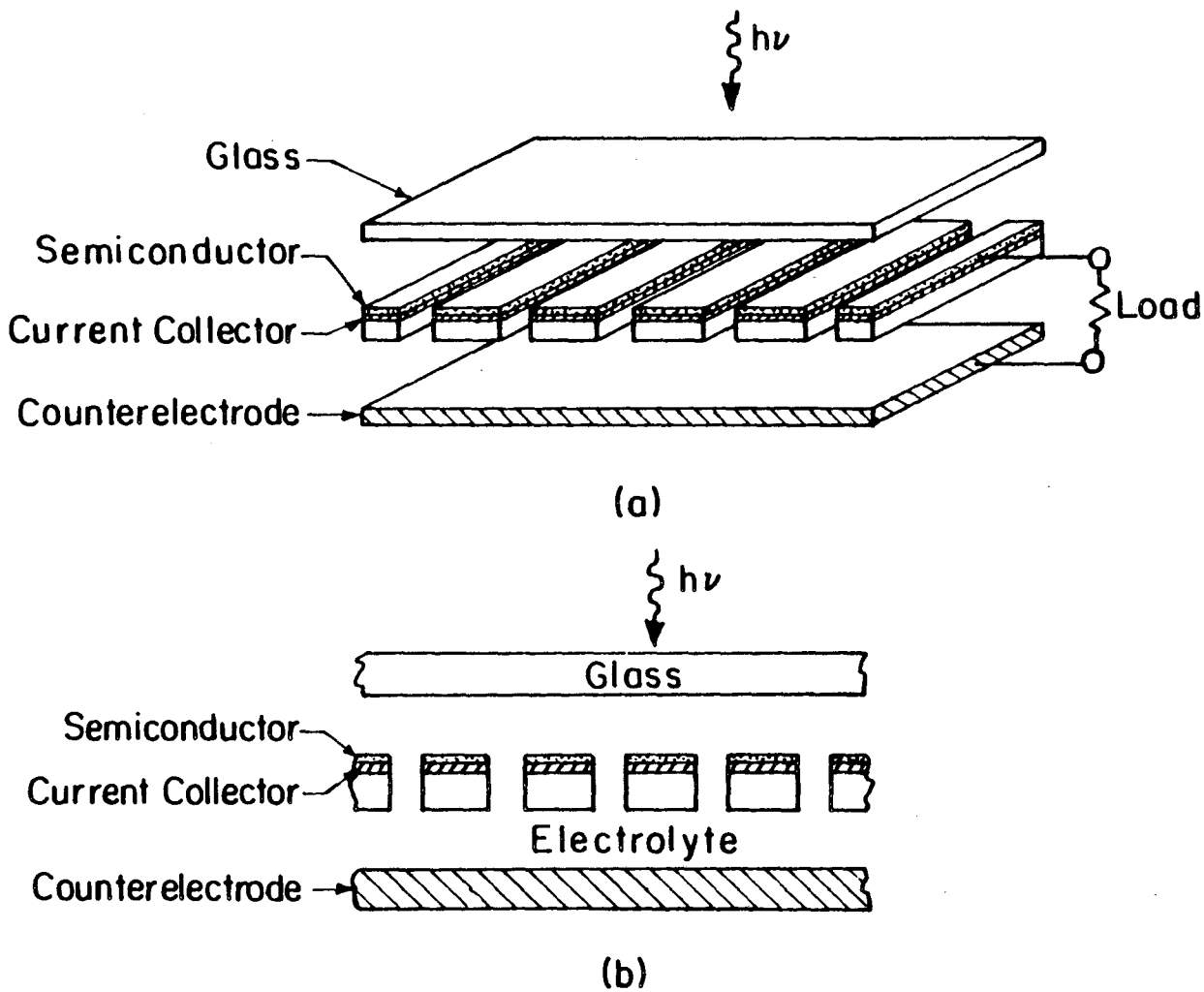

XBL 831-7974

Figure 4. Design of the liquid-junction photovoltaic cell. System 2: slotted semiconductor.

assembly was chosen to be 0.5 cm, and the semiconductor assembly thickness was assumed to be 0.1 cm. The primary resistance for this system is presented in Figure 5 as a function of L/D with h/G as a parameter. The maximum power density is presented in Figure 6 as a function of L/h with h/G as a parameter. L/h was varied by varying the half-length; h/G by varying the half-gap. The maximum power density for this system is obtained with a small gap. For h/G=0.5 (G=1cm), the maximum power density was 47.8 W/m^2, and the maximum power efficiency was 5.4 percent. The current density under maximum power conditions was 15 mA/cm^2 delivered at 477.6 mV. For h/G=10 (G=0.05cm), the maximum power density was 67.7 W/m^2, and the maximum power efficiency was 7.7 percent. At maximum power the current density was 15.2 mA/cm^2 delivered at 534.6 mV.

2.3. System 3: Back-Illuminated Semiconductor

A cell design is presented in Figure 7 in which the semiconductor is illuminated from the current-collector side. The semiconducting film is deposited on a pane of transparent conducting glass. A current-collecting grid is used to offset the low conductivity of the glass. The semiconductor is separated from the counterelectrode by a gap filled with electrolyte. This design could be used with a membrane within the gap, which would allow separation of reaction products at each of the electrodes.

The potential drop between the semiconductor and the current-collecting grid can be obtained through application of the general solution to the resistance of a rectangular conductor with arbitrarily placed electrodes presented by Moulton.[55,56]

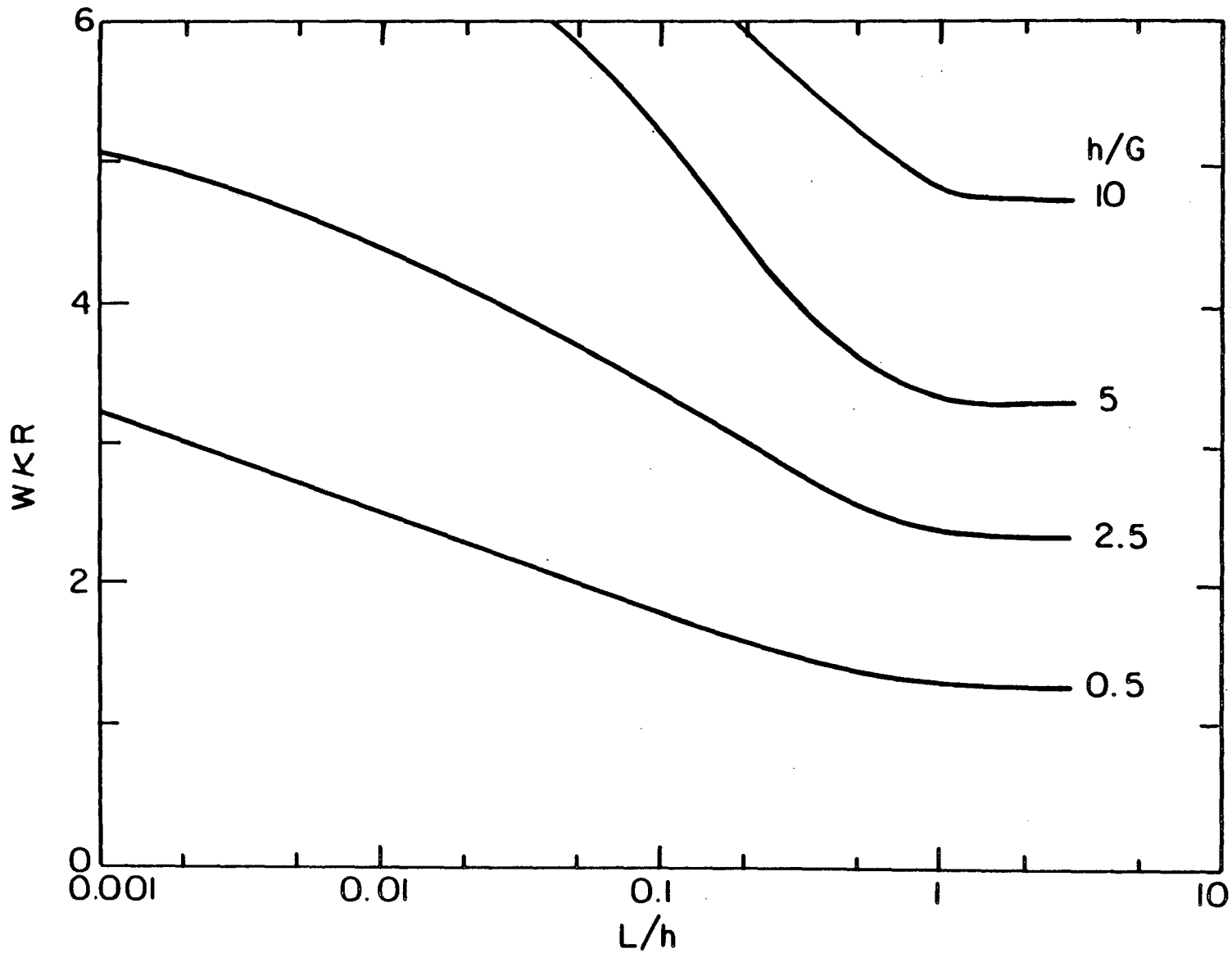

XBL 835-5618

Figure 5. Primary cell resistance as a function of L/h for system 2 with h/G as a parameter.

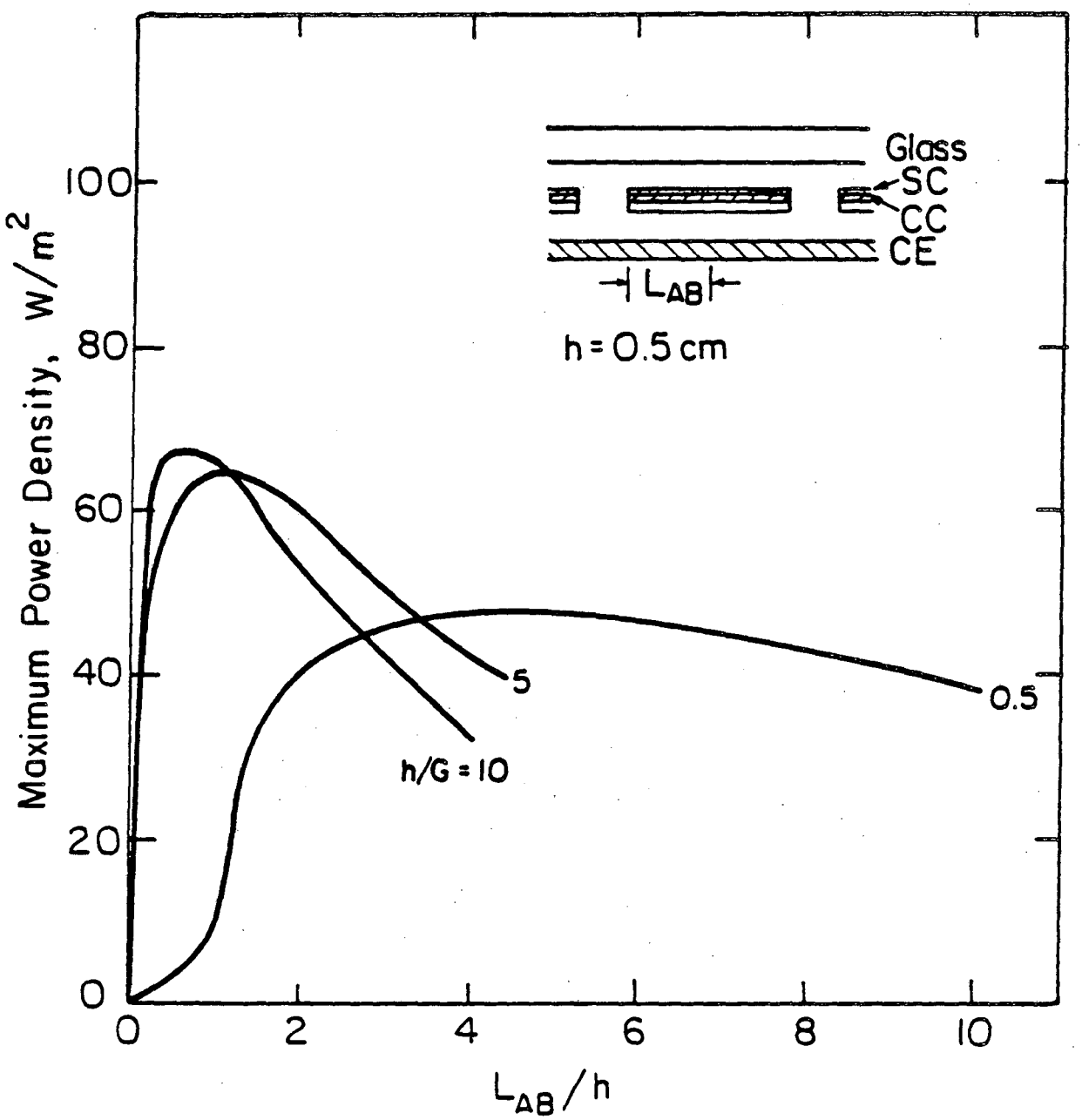

XBL 831-7975 A

Figure 6. Maximum power density as a function of L/h for system 2 with h/G as a parameter.

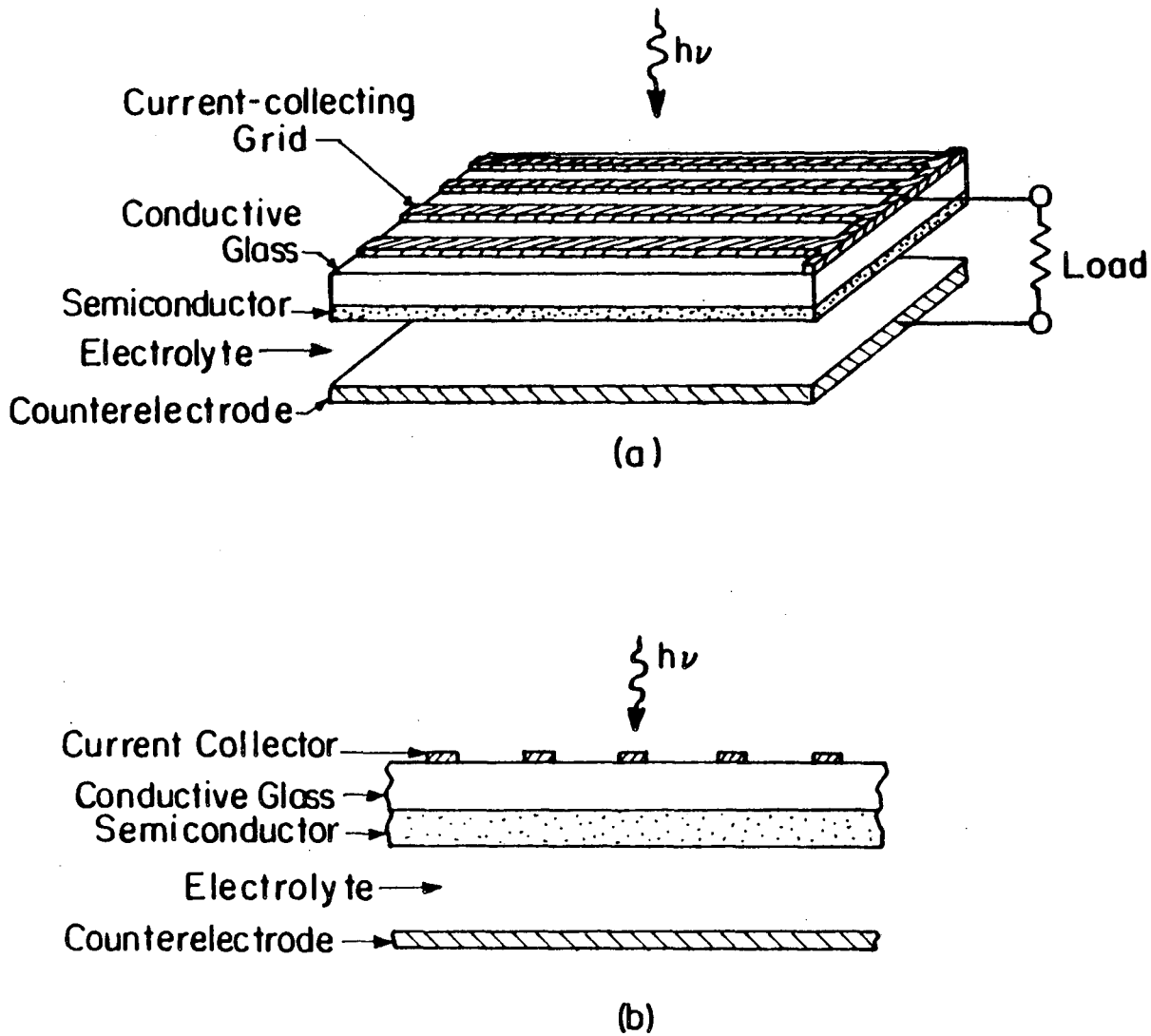

XBL 835-9615

Figure 7. Design of the liquid-junction photovoltaic cell. System 3: back-illuminated semiconductor.

The transparent conducting support for the semiconducting film was assumed to be SnO_2, which is commonly used as a transparent electrode. SnO_2 is a large band-gap semiconductor and is essentially transparent to light with energy below 3.7 eV. The properties of SnO_2 have been reviewed by Jarzebski and Marton.[57-59] The conductivity of the transparent material was assumed to be 50 mho/cm, and the total absorption and reflection losses at the air-SnO_2 interface for a 1/8 inch thick plate were assumed to be 8 percent. The reflectance at the SnO_2-GaAs interface was assumed to be 5 percent. The separation between the counterelectrode and the semiconductor was 0.5 cm.

The maximum power density is presented in Figure 8 as a function of the ratio of the current-collector-element spacing to the element width L/D. When L/D is equal to one, the semiconductor is completely blocked, and the power density is zero. When L/D is large, the resistance of the SnO_2 becomes important. The optimal value of L/D is around 100.; the maximum power density is 118.5 W/m^2, and the power efficiency is 13.4 percent. The current density under optimal operating conditions is 21.0 mA/cm^2 delivered at a cell potential of 564.3 mV.

The excellent performance of this cell design as compared to systems 1 and 2 can be misleading. Facilitated recombination at the semiconductor-metal interface was not included in the model. The back-illuminated system does have inherent advantages over front-illuminated cells. Optical losses, for example, can be smaller, and separation of electrochemical products is feasible. The relative rates of electron-hole recombination at the semiconductor-metal and the electrolyte-semiconductor interfaces, however, will influence the relative merit of front and back illumination.

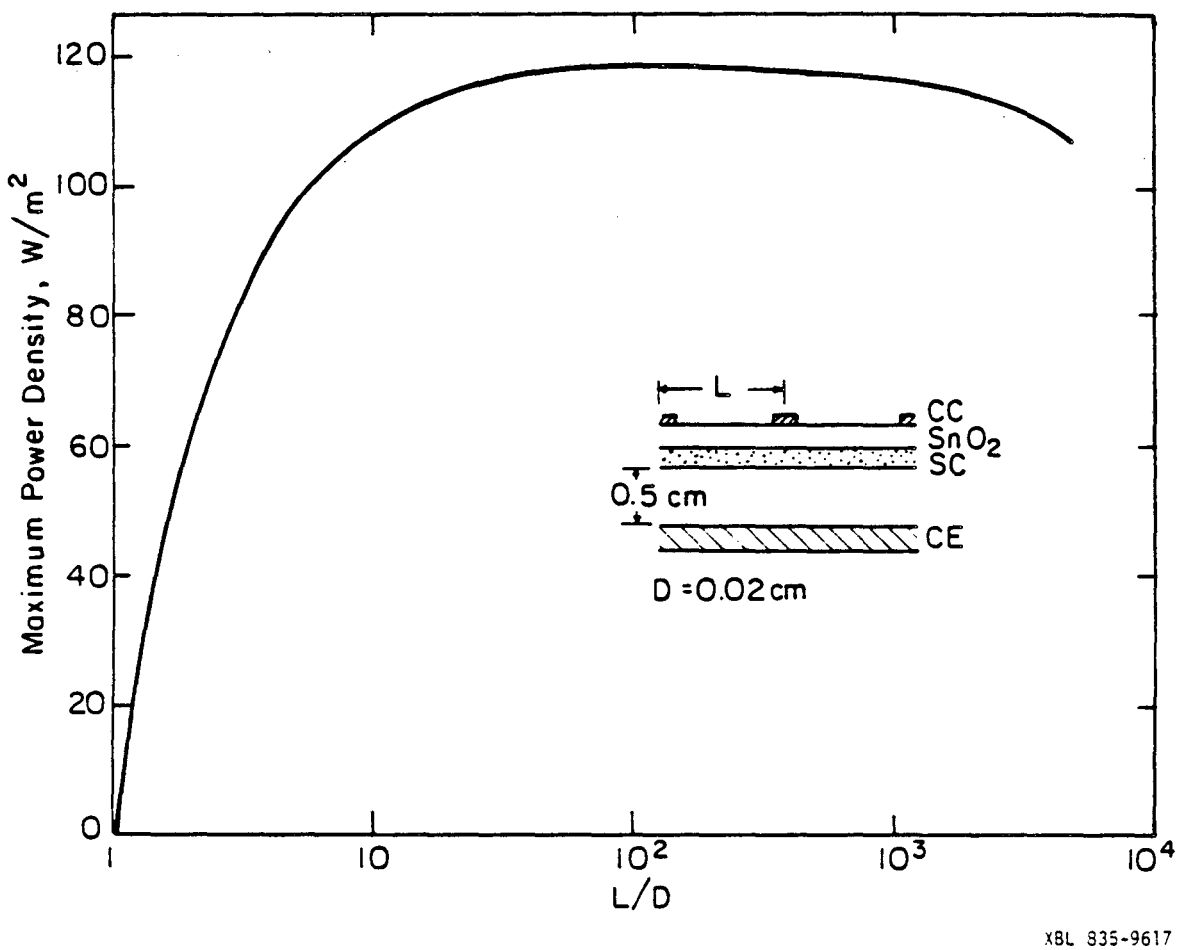

Figure 8. Maximum power density as a function of L/D for system 3 with a current-collector element thickness of 0.01 cm.

3. INTENSITY OF ILLUMINATION

The intensity of solar illumination varies with location, cloud cover, day of year, and time of day. In addition, mirrors and lenses can be used to concentrate the sunlight and reduce the amount of semiconducting material incorporated into the cell. The prediction of the performance of a given design of the liquid-junction photovoltaic cell must therefore consider the effect of the intensity of illumination.

The maximum power efficiency is presented as a function of illumination intensity in Figures 9, 10, and 11 for systems 1, 2, and 3, respectively. The cells were designed with the design parameters calculated to be optimal under AM-2 illumination. The power efficiency decreases with increasing illumination due to the influence of electrolyte resistance and kinetic and mass-transfer limitations at the counterelectrode. These phenomena become increasingly important as current densities increase, and mass-transfer limitations at the counterelectrode result in an upper limit for cell currents.

The maximum power efficiency for systems 2 and 3 without counterelectrode limitations is also presented in Figures 10 and 11. These results are appropriate for cells with porous counterelectrodes. A porous counterelectrode may not be feasible for system 1 because of the need in this system to pass sunlight through the counterelectrode. The efficiency still decreases with illumination intensity due to electrolyte resistance.

The maximum cell current obtained under large magnitudes of illumination depends upon the ratio of the counterelectrode area to the semiconductor area. This ratio must be large for liquid-junction photovoltaic cells designed for large intensities of illumination.

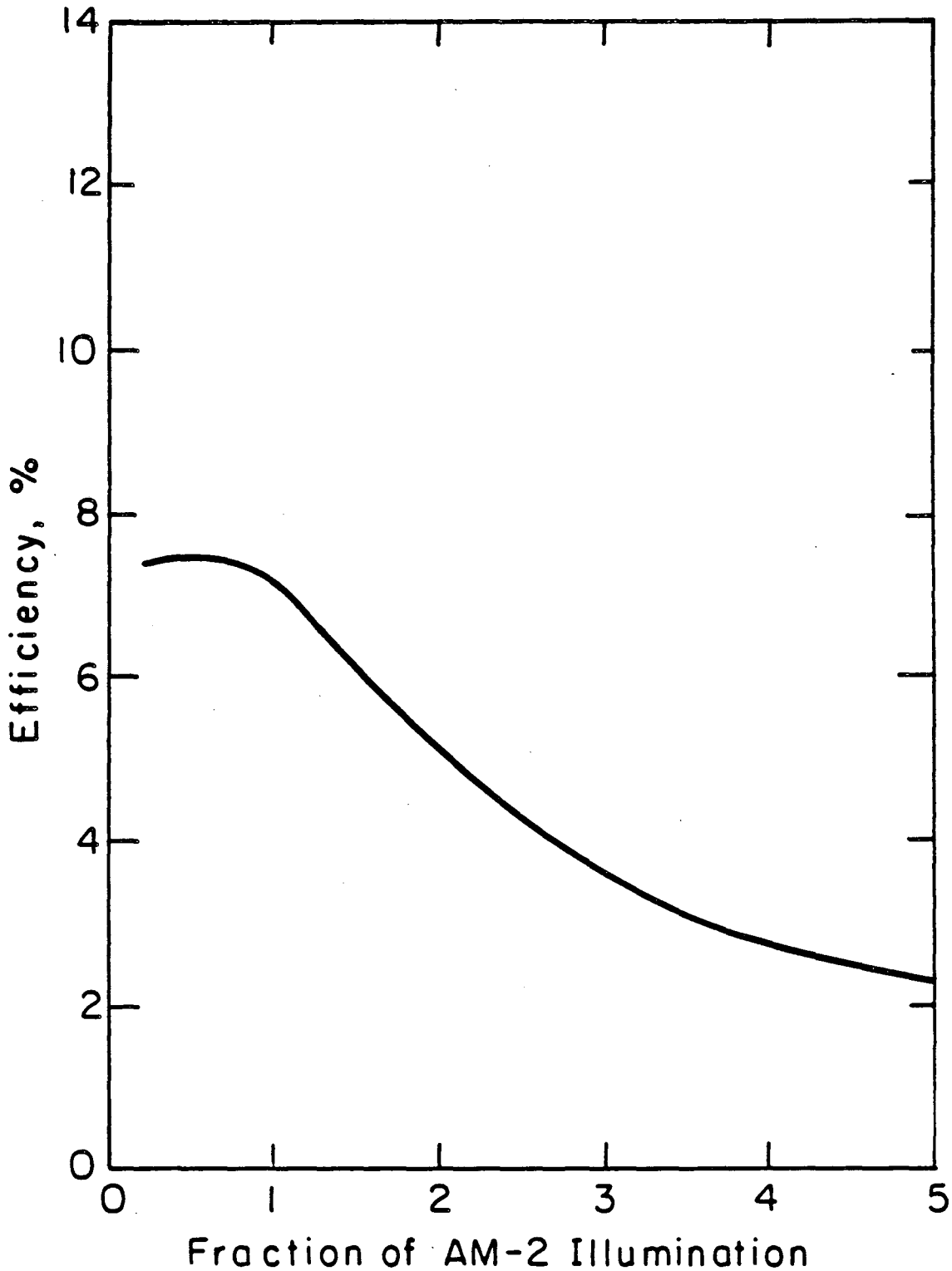

XBL 835-5614

Figure 9. Maximum power efficiency as a function of the fraction of AM-2 illumination (882 W/m^2) for system 1 with L/D = 14.

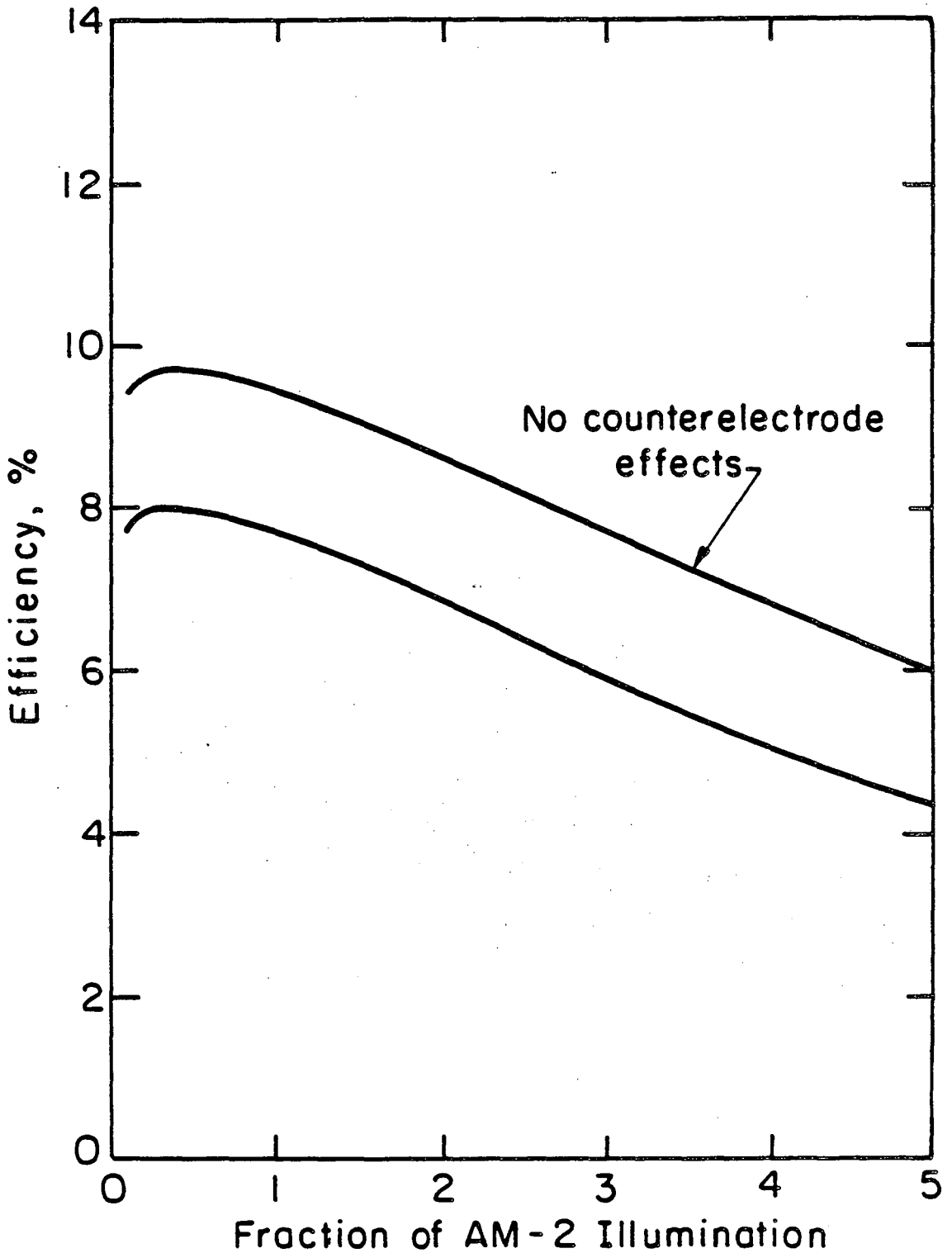

XBL835-5616

Figure 10. Maximum power efficiency as a function of the fraction of AM-2 illumination (882 W/m^2) for system 2 with h/G = 10 and L/h = 0.5.

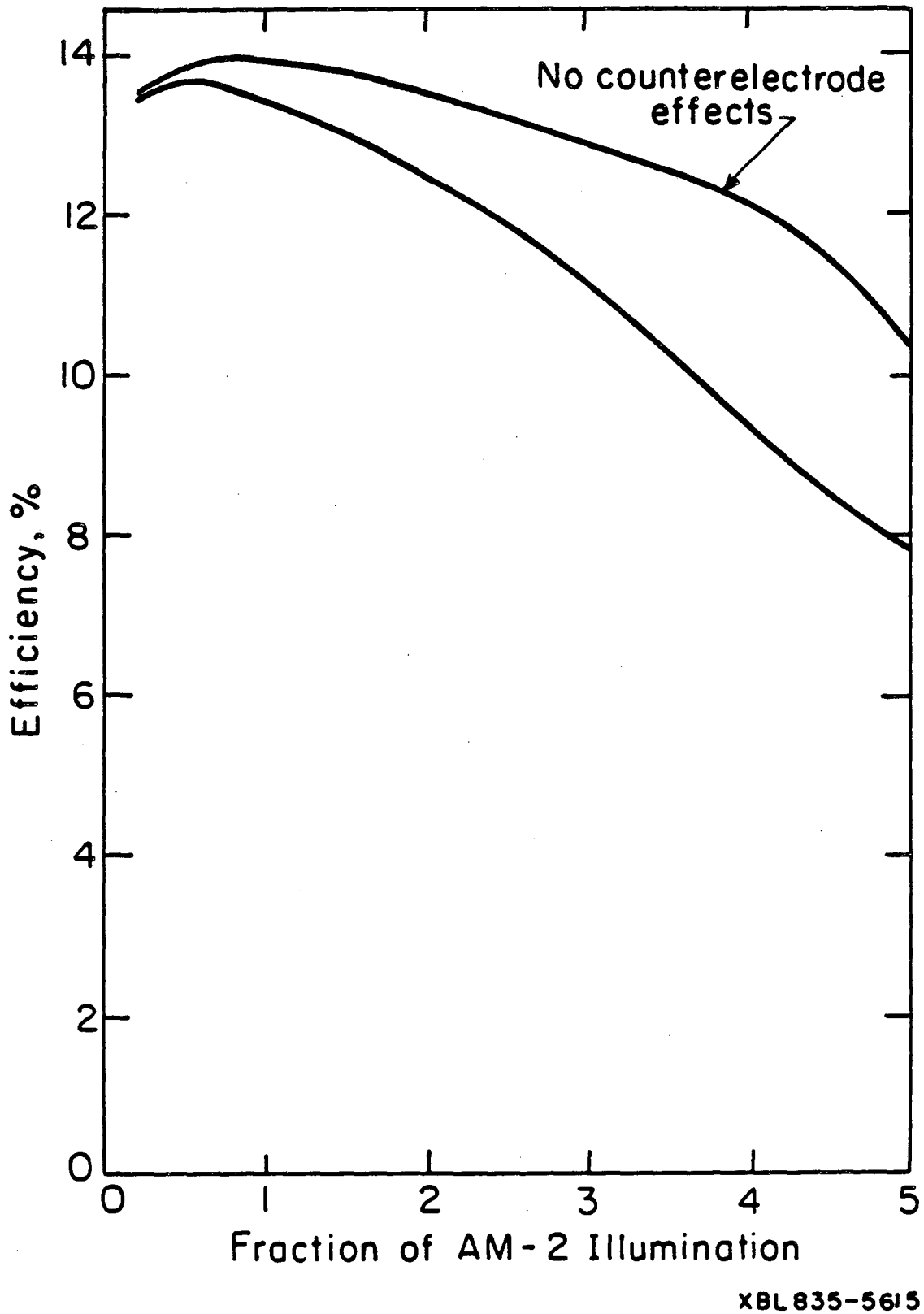

Figure 11. Maximum power efficiency as a function of the fraction of AM-2 illumination (882 W/m^2) for system 3 with a current-collector half width of 0.01 cm and with L/D = 100.

Replacement of the flat-plate counterelectrode with a porous electrode[60] can increase the counterelectrode area of systems 2 and 3. Inclusion of a cooling system in the cell design becomes important under these conditions. The electrolyte itself can serve as a heat exchange medium in photoelectrochemical systems.

4. DISCUSSION AND ECONOMIC ANALYSIS

The cells discussed in the previous sections can be divided into two groups, front and back illuminated, within which they can be compared fairly. The comparison of front and back illuminated cells depends upon the relative rates of recombination at the semiconductor-metal and electrolyte-semiconductor interfaces, and these rates will differ from one system to another.

The calculated power efficiencies are presented in Table 2 for the front-illuminated systems. Semiconductor effects, such as recombination, reduce the power efficiency from a value of 37 percent, based solely upon band gap, to 15.3 percent. Reflection losses, with an arbitrarily chosen 80 percent efficiency of illumination, reduce this value to 12.2 percent. This value can be compared to the 12 percent efficiency obtained in the experimental work of Heller and Miller.[8,40,41] The effect of cell design and illumination losses is to reduce the performance to 7.2 percent for system 1 and 7.7 percent for system 2.

The calculated power efficiencies are presented in Table 3 for the back-illuminated system. Semiconductor effects reduce the power efficiency from a value of 37 percent, based solely upon band gap, to 17.2 percent. Enhanced recombination at the semiconductor-current collector interface was not included in these calculations. The effect of cell design and

Table 2. Power Efficiency under Front-Illummination

	No Illumination Losses	Illumination Losses*	Experimental Results
Optimal Band Gap	45	36 (80%)	
GaAs Band Gap	37	30 (80%)	
Semiconductor-Electrolyte Junction	15.3	12.2 (80%)	12.0
Cell Design (1)	10.1	7.2 (55.4%)	
Cell Design (2)	9.8	7.7 (71.6%)	

* In some cases the number in parenthesis represents the fraction of AM-2 illumination (above the band gap) which actually enters the semiconductor, after accounting for reflection, shadowing, and absorption in the intervening phases. In other cases, where detailed calculations were not made, it represents the ratio to column 1 because the nonlinear effect of illumination could not be assessed.

Table 3. Power Efficiency under Back-Illumination

	No Illumination Losses	Illumination Losses*
Optimal Band Gap	45	36 (80%)
GaAs Band Gap	37	30 (80%)
Current Collector and Semiconductor-Electrolyte Junction	17.2	13.8 (80%)
Cell Design (3)	15.4	13.4 (86.5%)

* In some cases the number in parenthesis represents the fraction of AM-2 illumination (above the band gap) which actually enters the semiconductor, after accounting for reflection, shadowing, and absorption in the intervening phases. In other cases, where detailed calculations were not made, it represents the ratio to column 1 because the nonlinear effect of illumination could not be assessed.

illumination losses is to reduce the power efficiency to 13.4 percent.

The calculated performance could be improved by making distances between semiconductor and counterelectrode smaller, reducing the effect of electrolyte resistance. The values chosen for this analysis were based primarily on mechanical considerations. A spacing of 0.5 cm was used between all cell elements. A smaller spacing could result in shorting of

counterelectrode and semiconductor and/or trapping of gas bubbles. The influence of the counterelectrode could be reduced by increasing the flow rate or degree of mixing near the counterelectrode, thereby increasing the limiting current. Kinetic limitations at the semiconductor-electrolyte interface were not considered here and may greatly reduce the performance of some semiconductor systems.

Current-potential curves are presented in Figure 12 for the front-illuminated cells. The optimally designed cells of systems 1 and 2 are compared to the cell without interfacial kinetic limitations, counterelectrode limitations, and electrolytic resistance. The cell with a slotted semiconductor has a larger power efficiency than the wire-grid counterelectrode cell and can be designed for separation of chemical products. The analysis of the system designed for separation of chemical products would include the electrical resistance of the membrane.

Current-potential curves are presented in Figure 13 for the back-illuminated cell. The optimally designed cell of systems 3 is compared to the cell without interfacial kinetic limitations, counterelectrode limitations, and electrolytic resistance. The back-illuminated design is appealing because chemical products can be separated and because of reduced losses of illumination.

The following discussion of cell economics is appropriate for all photovoltaic devices. The allowable capital investment for the cell is given by

$$I = 8.76\ P_{in}\ \eta\ \Delta c\ y_e\ , \tag{15}$$

where P_{in} is the annual incident illumination intensity averaged over 24 hours in W/m^2, η is the cell efficiency, Δc is the difference in selling price

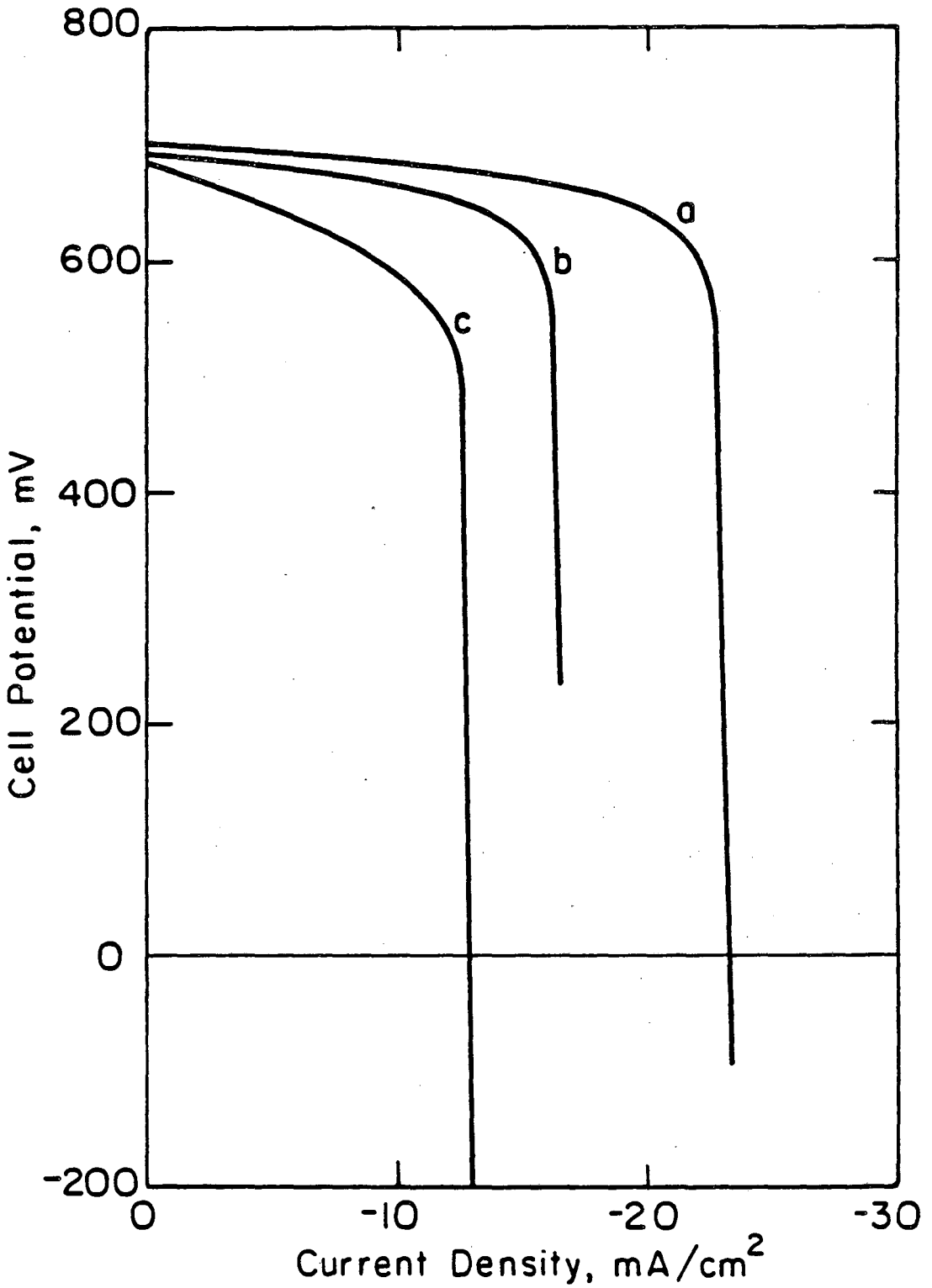

XBL 835-5612

Figure 12. Cell potential as a function of current density for (a) a front-illuminated semiconductor without kinetic, electrolyte-resistance and counterelectrode limitations; (b) system 1 with a counter-electrode element diameter of 0.10 cm and with L/D = 14; and (c) system 2 with h/G = 10 and L/h = 0.5.

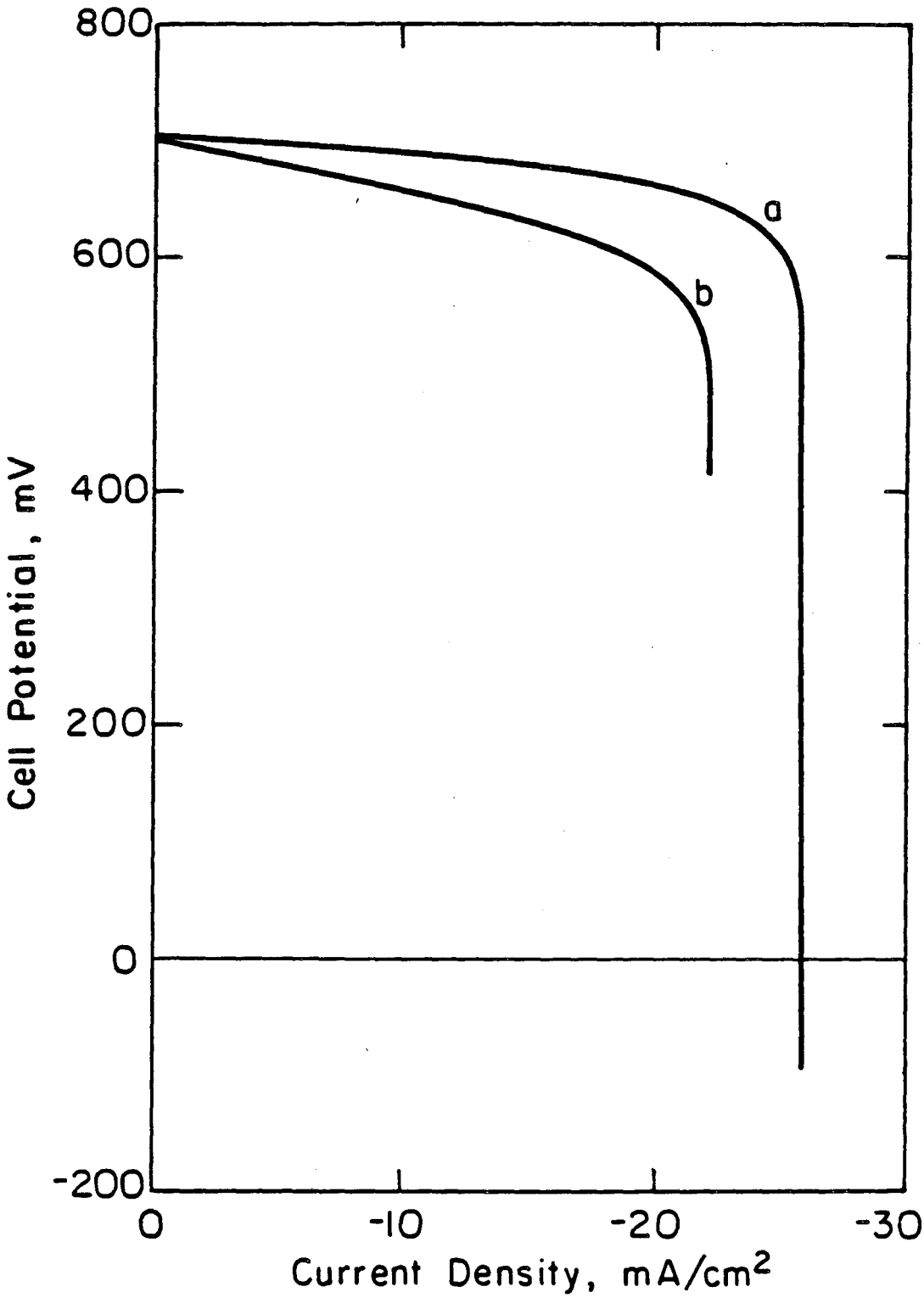

XBL 835-5613

Figure 13. Cell potential as a function of current density for (a) a back-illuminated semiconductor without kinetic, electrolyte-resistance and counterelectrode limitations; and (b) system 3 with a current-collector element half-thickness of 0.01 cm and with L/D = 100.

and operating cost in dollars/kW-hr, and y_e is the break-even point in years. This equation is presented as a nomogram in Figure 14. The power output of the liquid-junction cell is presented in Figure 14a as a function of the incident solar illumination with the average efficiency of the device as a parameter. The incident solar illumination is averaged over a 24 hour period. On this basis, the average insolation of the continental United States is 200 to 250 W/m^2.[11] Lenses or mirrors could be used to increase the amount of sunlight striking the semiconductor surface. The annual return on investment is presented in Figure 14b as a function of the power output with power cost as a parameter. The total initial investment is presented in Figure 14c as a function of the averaged annual investment with cell break-even period as a parameter.

Based upon a 7.7 percent power efficiency (averaged over 24 hours), 250 W/m^2 incident illumination (averaged over 24 hours), 0.05 dollars/kW-hr profit, and a break-even period of 5 years, an investment of 42 dollars/m^2 is justified for the complete cell. Based upon a 13.4 percent power efficiency (averaged over 24 hours), an investment of 73 dollars/m^2 is justified for the complete cell.

An increase of solar illumination by a factor of five while reducing the efficiency to 6 percent (system 2 with a porous counterelectrode) yields an acceptable initial investment of 164 dollars/m^2. An efficiency of 10.4 percent (system 3 with a porous counterelectrode) yields an acceptable initial investment of 285 dollars/m^2. If the mirrors and lenses needed to concentrate sunlight are cheaper than the semiconducting film, the cell may be most economical under high illumination. Maintenance of a high efficiency under high illumination is possible only with the back-illuminated

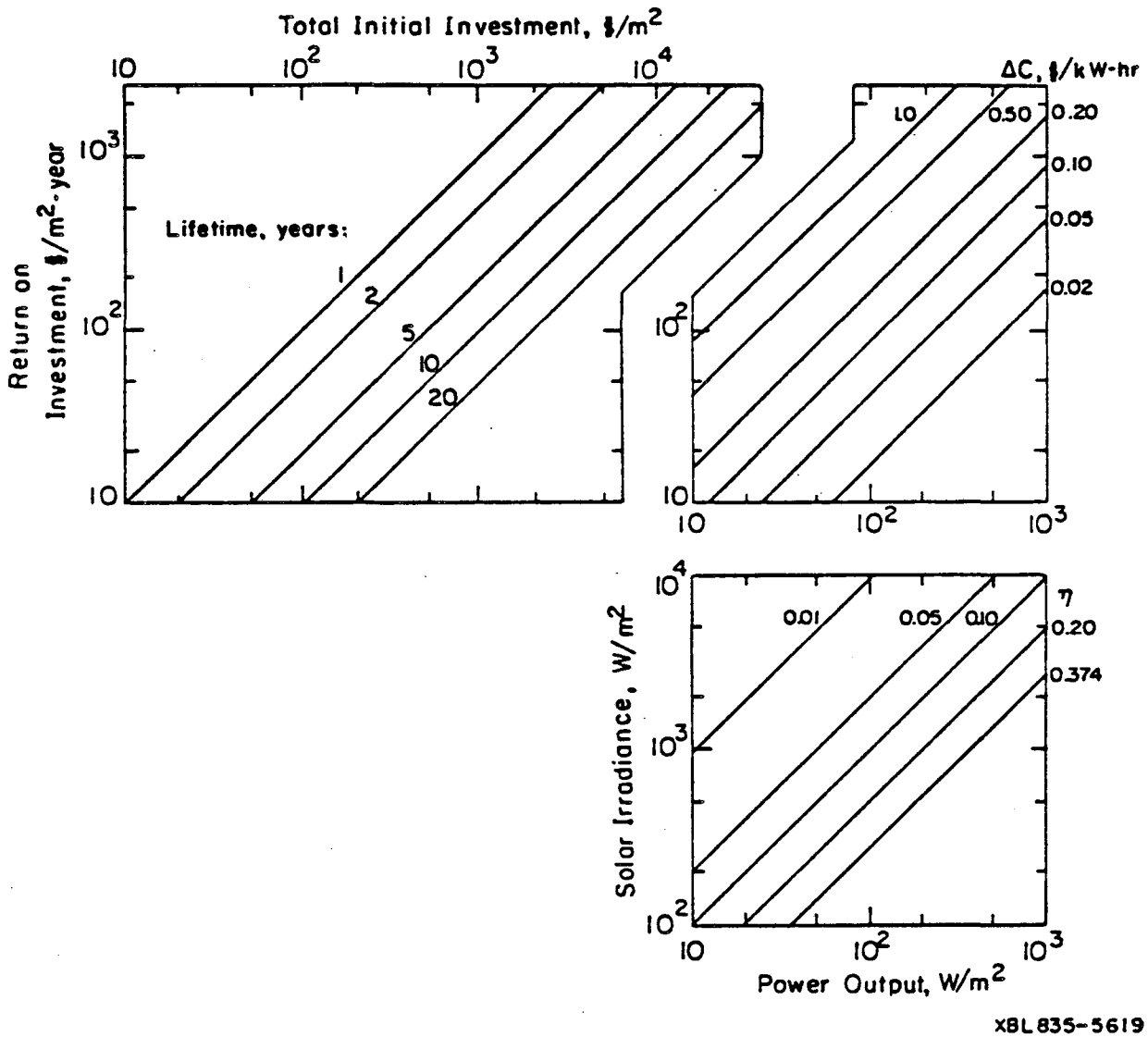

Figure 14. Economic analysis of the liquid-junction photovoltaic cell; (a) power output as a function of the incident solar illumination with power efficiency as a parameter; (b) averaged annual return on investment as a function of the power output with power cost as a parameter; (c) total initial investment as a function of averaged annual return on investment with cell lifetime as a parameter.

cell of Figure 7 and the front-illuminated cell of Figure 4, both coupled with porous counterelectrodes.

The values presented here can be compared to the estimate presented by Weaver *et al.*[61] of 0.34 dollars per peak watt. This estimate is based on materials cost and assumes a cell efficiency of 13 percent. Under AM-2 illumination, this value corresponds to 39 dollars/m^2.

5. CONCLUSIONS

The optimization of the liquid-junction photovoltaic cell depends upon the choice of semiconductor, electrolyte, and cell design. The system studied in this work, n-GaAs with a Se_2^{-2}/Se^{-2} redox couple, is close to optimal with respect to utilization of solar irradiation and therefore provides a best-case estimate of liquid-junction cell efficiency. This system, however, exhibits a small rate of corrosion under illumination (a few micrometers per year).[62]

The performance of the liquid-junction photovoltaic cell is strongly dependent upon the design, surface area, and placement of the counterelectrode and current collectors. This system may be economical under concentrated illumination or where the power produced has high value.

6. REFERENCES

[1] Fujishima, Akira, and Kenichi Honda, "Electrochemical Photolysis of Water at a Semiconductor Electrode," *Nature*, *238* (1972), 37-38.

[2] Manassen, J., D. Cahen, and G. Hodes, "Electrochemical, Solid State, Photochemical, and Technological Aspects of Photoelectrochemical Energy Converters," *Nature*, *263* (1976), 97-100.

[3] Bard, Allen J., "Photoelectrochemistry and Heterogeneous Photocatalysis at Semiconductors," *Journal of Photochemistry*, *10* (1979), 59-75.

[4] Ehrenreich, H. and J. H. Martin, "Solar Photovoltaic Energy," *Physics Today*, *32*, 9 (1979), 25-32.

[5] Wrighton, Mark S., "Photoelectrochemical Conversion of Optical Energy to Electricity and Fuels," *Accounts of Chemical Research*, *12* (1979), 303-310.

[6] Gerischer, Heinz, "Heterogeneous Electrochemical Systems for Solar Energy Conversion," *Pure and Applied Chemistry*, *52* (1980), 2649-2667.

[7] Bard, Allen J., "Photoelectrochemistry," *Science*, *207* (1980), 139-144.

[8] Heller, Adam, "Conversion of Sunlight into Electrical Power and Photoassisted Electrolysis of Water in Photoelectrochemical Cells," *Accounts of Chemical Research*, *14* (1981), 154-162.

[9] Green, Mino, "Electrochemistry of the Semiconductor-Electrolyte Interface," Chapter 5 in *Modern Aspects of Electrochemistry*, Volume 2, J. O'M Bockris, editor, Academic Press Inc., New York, 1959.

[10] Gerischer, Heinz, "Semiconductor Electrode Reactions," Chapter 4 in *Advances in Electrochemistry and Electrochemical Engineering*, Volume 1, Paul Delahay, editor, Interscience Publishers, New York, 1961.

[11] Archer, M.D., "Electrochemical Aspects of Solar Energy Conversion," *Journal of Applied Electrochemistry*, *5* (1975), 17-38.

[12] Rajeshwar, K., P. Singh, and J. DuBow, "Energy Conversion in Photoelectrochemical Systems: A review," *Electrochimica Acta*, *23* (1975), 1117-1144.

[13] Harris, L. A., and R. H. Wilson, "Semiconductors for Photoelectrolysis," *Annual Reviews in Materials Science*, *8* (1978), 99-134.

[14] Nozik, Arthur, J., "Photoelectrochemistry: Applications to Solar Energy Conversion," *Annual Reviews in Physical Chemistry*, *29* (1978), 189-222.

[15] Tomkiewicz, M., and H. Fay, "Photoelectrolysis of Water with Semiconductors," *Applied Physics*, *18* (1979), 1-28.

[16] Wilson, R.H., "Electron Transfer Processes at the Semiconductor-

Electrolyte Interface," *CRC Critical Reviews in Solid State and Materials Science*, (1980), 1-41.

[17] Memming, R., "Solar Energy Conversion by Photoelectrochemical Processes," *Electrochimica Acta*, *25* (1980), 77-88.

[18] Morrison, S. Roy, *Electrochemistry at Semiconductor and Oxidized Metal Electrodes*, Plenum Press, New York, 1980.

[19] Khan, Shahed U. M., and John O'M. Bockris, "Photoelectrochemical Kinetics and Related Devices," Chapter 3 in *Modern Aspects of Electrochemistry*, Volume 14, J. O'M. Bockris, B. E. Conway, and R. E. White, editors, Plenum Press, New York, 1982.

[20] Orazem, Mark Edward, *Mathematical Modeling and Optimization of Liquid-Junction Photovoltaic Cells*, PhD thesis, University of California, Berkeley, June, 1983 (LBL-16131).

[21] Orazem, Mark E. and John Newman, "Mathematical Modeling of Liquid-Junction Photovoltaic Cells: I. Governing Equations," submitted to *the Journal of the Electrochemical Society*, (LBL-16210).

[22] Oman, Henry, and Joseph W. Gelzer, "Solar Cells and Arrays," in *Energy Technology Handbook*, Douglas M. Considine, editor, McGraw Hill, New York, 1977, 6.56-6.80.

[23] Loferski, Joseph J., "Theoretical Considerations Governing the Choice of the Optimum Semiconductor for Photovoltaic Solar Energy Conversion," *Journal of Applied Physics*, *27* (1956), 777-784.

[24] Loferski, Joseph J., "Recent Research on Photovoltaic Solar Energy Converters," *Proceedings of the IEEE*, (1963) 667-674.

[25] Wysocki, J. J., "Photon Spectrum Outside the Earth's Atmosphere," *Solar Energy*, *6* (1962) 104.

[26] Wolf, M., "Limitations and Possibilities for Improvement of Photovoltaic Solar Energy Converters, Part I: Considerations for Earth's Surface Operation," *Proceedings of the IRE*, *48* (1960), 1246-1263.

[27] Shockley, William, and Hans J. Queisser, "Detailed Balance Limit of Efficiency of p-n Junction Solar Cells," *Journal of Applied Physics*, *32* (1961), 510-519.

[28] Chang, K. C., A. Heller, B. Schwartz, S. Menezes, and B. Miller, "Stable Semiconductor Liquid-Junction Cell with 9% Solar to Electrical Conversion Efficiency," *Science*, *196* (1977), 1097-1098.

[29] Heller, Adam, Barry Miller, and F. A. Thiel, "11.5 % Solar Conversion Efficiency in the Photocathodically Protected p-InP/V^{3+}-V^{2+}-HCl Semiconductor Liquid-Junction Cell," *Applied Physics Letters*, *38* (1981), 282-284.

[30] Gerischer, Heinz, "Photoelectrochemical Solar Cells," in *Proceedings of the 2nd Electrochemical Photovoltaic Solar Energy Conference*, R. van Overstraeten and W. Palz, editors, D. Reidel, Boston, 1979, 408-431.

[31] Menezes, S., A. Heller, and B. Miller, "Metal Filmed-Semiconductor Photoelectrochemical Cells," *Journal of the Electrochemical Society*, *127* (1980), 1268-1273.

[32] Frese, K. W., Jr., M. J. Madou, and S. R. Morrison, "Investigation of Photoelectrochemical Corrosion of Semiconductors: III. Effects of Metal Layers on the Stability of GaAs," *Journal of the Electrochemical Society*, *128* (1981), 1939-1943.

[33] Noufi, Rommel, Dennis Tench, and Leslie F. Warren, "Protection of n-GaAs Photoanodes with Photoelectrochemically Generated Polypyrrole Films," *Journal of the Electrochemical Society*, *127* (1980), 2310-2311.

[34] Noufi, Rommel, Dennis Tench, and Leslie F. Warren, "Protection of Semiconductor Photoanodes with Photoelectrochemically Generated Polypyrrole Films," *Journal of the Electrochemical Society*, *128* (1981), 2596-2599.

[35] Skotheim, Terje, Ingemar Lundstrom, and Jiri Prejza, "Stabilization of n-Si Photoanodes to Surface Corrosion in Aqueous Electrolyte with a Thin Film of Polypyrrole," *Journal of the Electrochemical Society*, *128* (1981), 1625-1626.

[36] Fan, Fu-Ren F., Bob L. Wheeler, Allen J. Bard, and Rommel N. Noufi, "Semiconductor Electrodes XXXIX. Techniques for Stabilization of n-Silicon Electrodes in Aqueous Solution Photoelectrochemical Cells," *Journal of the Electrochemical Society*, *128* (1981), 2042-2045.

[37] Bull, Randy A., Fu-Ren F. Fan, Allen J. Bard, "Polymer Films on Electrodes VII. Electrochemical Behavior at Polypyrrole-Coated Platinum and Tantalum Electrodes," *Journal of the Electrochemical Society*, *129* (1982), 1009-1015.

[38] Skotheim, Terje, L.-G. Petersson, O. Inganas, and Ingemar Lundstrom, "Photoelectrochemical Behavior of n-Si Electrodes Protected with Pt-Polypyrrole," *Journal of the Electrochemical Society*, *129* (1982), 1737-1741.

[39] White, Henry S., Hector D. Abruna, and Allen J. Bard, "Semiconductor Electrodes XLI. Improvement of Performance of n-WSe_2 Electrodes by Electrochemical Polymerization of o-Phenylenediamine at Surface Imperfections," *Journal of the Electrochemical Society*, *129* (1982), 265-271.

[40] Heller, Adam, and B. Miller, "Photoelectrochemical Solar Cells: Chemistry of the Semiconductor-Liquid Junction," Chapter 12 in *Interfacial Photoprocesses: Energy Conversion and Synthesis*, *Advances in Chemistry Series*, *184*, Mark S. Wrighton, editor, American Chemical Society, Washington D. C., 1980.

[41] Parkinson, B. A., A. Heller, and B. Miller, "Enhanced

Photoelectrochemical Solar-Energy Conversion by Gallium-Arsenide Surface Modification," *Applied Physics Letters*, *33* (1978), 521-523.

[42] Chang, K. C., A. Heller, B. Schwartz, S. Menezes, and B. Miller, "Stable Semiconductor Liquid-Junction Cell with 9% Solar to Electrical Conversion Efficiency," *Science*, *196* (1977), 1097-1098.

[43] Orazem, Mark E. and John Newman, "Mathematical Modeling of Liquid-Junction Photovoltaic Cells: II. Effect of System Parameters on Current-Potential Curves," submitted to *the Journal of the Electrochemical Society*, (LBL-16211).

[44] Hovel, Harold J., "Solar Cells," Volume 11 of *Semiconductors and Semimetals*, R. K. Willardson and Albert C. Beer, editors, Academic Press, New York, 1975.

[45] Iles, P. A., "Evolution of Silicon Solar Cell Design," *9th IEEE Photovoltaic Specialists Conference*, Silver Springs, MD, 1972, 1-5.

[46] Parkinson, Bruce, "An Evaluation of Various Configurations for Photoelectrochemical Photovoltaic Solar Cells," *Solar Cells*, *6* (1982), 177-189.

[47] Mitchell, Kim W., "Status of New Thin-Film Photovoltaic Technologies," *Annual Reviews in Materials Science*, *12* (1982), 401-415.

[48] Fleck, R. N., D. N. Hanson, and C. W. Tobias, "Numerical Evaluation of Current Distribution in Electrochemical Systems," *Lawrence Berkeley Laboratory Report*, UCRL-11612, 1964.

[49] Kasper, Charles, "The Theory of the Potential and the Technical Practice of Electrodeposition: I. The General Problem and the Cases of Uniform Flow," *Transactions of the Electrochemical Society*, *77* (1940), 353-363.

[50] Kasper, Charles, "The Theory of the Potential and the Technical Practice of Electrodeposition: II. Point-Plane and Line-Plane Systems," *Transactions of the Electrochemical Society*, *77* (1940), 365-384.

[51] Kasper, Charles, "The Theory of the Potential and the Technical Practice of Electrodeposition: III. Linear Polarization on Some Line-Plane Systems," *Transactions of the Electrochemical Society*, *78* (1940), 131-146.

[52] Kasper, Charles, "The Theory of the Potential and the Technical Practice of Electrodeposition: IV. The Flow Between and to Circular Cylinders," *Transactions of the Electrochemical Society*, *78* (1940), 147-161.

[53] Kasper, Charles, "The Theory of the Potential and the Technical Practice of Electrodeposition: V. The Two-Dimensional Rectangular Enclosures," *Transactions of the Electrochemical Society*, *82* (1942), 153-185.

[54] Orazem, Mark E. and John Newman, "Primary Current Distribution and Resistance of a Slotted-Electrode Cell," submitted to *the Journal of the*

Electrochemical Society, (LBL-15294).

[55] Moulton, H. Fletcher, "Current Flow in Rectangular Conductors," *Proceedings of the London Mathematical Society (Ser. 2)*, *3* (1905), 104-110.

[56] Bowman, F., *Introduction to Elliptic Functions with Applications*, John Wiley and Sons, Inc., New York, 1953.

[57] Jarzebski, Z. M., and J. P. Marton, "Physical Properties of SnO_2 Materials: I. Preparation and Defect Structure," *Journal of the Electrochemical Society*, *123* (1976), 199C-205C.

[58] Jarzebski, Z. M., and J. P. Marton, "Physical Properties of SnO_2 Materials: II. Electrical Properties," *Journal of the Electrochemical Society*, *123* (1976), 299C-310C.

[59] Jarzebski, Z. M., and J. P. Marton, "Physical Properties of SnO_2 Materials: III. Optical Properties," *Journal of the Electrochemical Society*, *123* (1976), 333C-346C.

[60] Canfield, Duane, and S. Roy Morrison, "Electrochemical Storage Cell Based on Polycrystalline Silicon," *Laurence Berkeley Laboratory Report*, LBL-14639, 1982.

[61] Weaver, N. L., R. Singh, K. Rajeschwar, P. Singh, and J. DuBow, "Economic Analysis of Photoelectrochemical Cells," *Solar Cells*, *3* (1981), 221-232.

[62] Wrighton, Mark S., Jeffrey M. Bolts, Andrew B. Bocarsly, Michael C. Palazzotto, and Erick G. Walton, "Stabilization of n-Type Semiconductors to Photoanodic Dissolution: II-VI and III-V Compound Semiconductors and Recent Results for n-Type Silicon," *Journal of Vacuum Science Technology*, *15* (1978), 1429-1435.

This report was done with support from the Department of Energy. Any conclusions or opinions expressed in this report represent solely those of the author(s) and not necessarily those of The Regents of the University of California, the Lawrence Berkeley Laboratory or the Department of Energy.

Reference to a company or product name does not imply approval or recommendation of the product by the University of California or the U.S. Department of Energy to the exclusion of others that may be suitable.

TECHNICAL INFORMATION DEPARTMENT
LAWRENCE BERKELEY LABORATORY
UNIVERSITY OF CALIFORNIA
BERKELEY, CALIFORNIA 94720